

UC Irvine

UC Irvine Previously Published Works

Title

Thrombospondin-4 divergently regulates voltage-gated Ca²⁺ channel subtypes in sensory neurons after nerve injury

Permalink

<https://escholarship.org/uc/item/4h48p0k5>

Journal

Pain, 157(9)

ISSN

0304-3959

Authors

Pan, Bin
Guo, Yuan
Wu, Hsiang-En
[et al.](#)

Publication Date

2016-09-01

DOI

10.1097/j.pain.0000000000000612

Peer reviewed



Published in final edited form as:

Pain. 2016 September ; 157(9): 2068–2080. doi:10.1097/j.pain.0000000000000612.

Thrombospondin-4 divergently regulates voltage gated Ca^{2+} channel subtypes in sensory neurons after nerve injury

Bin Pan¹, Yuan Guo¹, Hsiang-En Wu¹, John Park³, Van Nancy Trinh², Z. David Luo^{2,3}, and Quinn H. Hogan¹

¹Department of Anesthesiology, Medical College of Wisconsin, 8701 Watertown Plank Road, Milwaukee, WI 53226

²Department of Anesthesiology & Perioperative Care, University of California Irvine, Irvine, CA 92697

³Department of Pharmacology, University of California Irvine, Irvine, CA 92697

Abstract

Loss of high-voltage-activated (HVA) calcium current (I_{Ca}) and gain of low-voltage-activated (LVA) I_{Ca} after painful peripheral nerve injury cause elevated excitability in sensory neurons. Nerve injury is also accompanied by increased expression of the extracellular matrix glycoprotein thrombospondin-4 (TSP4), and interruption of TSP4 function can reverse or prevent behavioral hypersensitivity following injury. We therefore investigated TSP4 regulation of I_{Ca} in dorsal root ganglion (DRG) neurons. During depolarization adequate to stimulate HVA I_{Ca} , TSP4 decreases both N- and L-type I_{Ca} and the associated intracellular calcium transient. In contrast, TSP4 increases I_{Ca} and the intracellular calcium signal following low voltage depolarization, which we confirmed is due to I_{Ca} through T-type channels. These effects are blocked by gabapentin, which ameliorates neuropathic pain by targeting the $\alpha_2\delta_1$ calcium subunit. Injury-induced changes of HVA and LVA I_{Ca} are attenuated in TSP4 knockout mice. In the neuropathic pain model of spinal nerve ligation, TSP4 application did not further regulate I_{Ca} of injured DRG neurons. Taken together, these findings suggest that elevated TSP4 following peripheral nerve injury may contribute to hypersensitivity of peripheral sensory systems by decreasing HVA and increasing LVA in DRG neurons via targeting the $\alpha_2\delta_1$ calcium subunit. Controlling TSP4 overexpression in peripheral sensory neurons may be a target for analgesic drug development for neuropathic pain.

Keywords

Neuropathic pain; Voltage-gated calcium channels; Thrombospondin-4

Corresponding author: Quinn H. Hogan M.D., Department of Anesthesiology, Medical College of Wisconsin, 8701 Watertown Plank Road, Milwaukee, WI 53226, Phone: 414-955-5727, Fax: 414-955-6507, qhogan@mcw.edu.

Conflict of interest statement

The authors have no conflicts of interest to declare.

1. Introduction

Sensory neurons possess a variety of voltage-gated calcium channel (VGCC) subtypes. High-voltage activated (HVA) VGCCs, including L-type ($Ca_v1.1$, $Ca_v1.2$, $Ca_v1.3$, and $Ca_v1.4$), P/Q-type ($Ca_v2.1$), N-type ($Ca_v2.2$) and R-type ($Ca_v2.3$) [65], require a strong depolarization for activation, and show minimal (L- and P-/Q- type) or moderate (N- and R-type) inactivation during sustained depolarization. In contrast, low-voltage activated (LVA) I_{Ca} , also known as T-type ($Ca_v3.1$, $Ca_v3.2$, $Ca_v3.3$) [65], is activated by weak depolarization and inactivates rapidly during sustained depolarization. Whereas HVA currents provide the Ca^{2+} influx that triggers feedback suppression of neuronal excitability through activation of Ca^{2+} -sensitive K^+ currents [68], LVA VGCCs directly contribute to burst firing and neuronal subthreshold membrane oscillatory activity [43; 59]. We have previously observed that peripheral nerve injury by chronic constriction injury (CCI) and spinal nerve ligation (SNL) decreases I_{Ca} in the somata of primary afferent neurons that reside in the dorsal root ganglia (DRGs) proximal to the site of injury [33; 53; 54]. Although studies from our and other labs show that extracellular signal-regulated kinase (ERK), Ca^{2+} /calmodulin-dependent protein kinase (CaMKII) and protein kinase C might modulate those calcium currents [37; 73; 77], the signaling pathway that initiates post-injury I_{Ca} loss is still unclear.

Thrombospondins (TSP) are a family of large oligomeric, extracellular matrix glycoproteins that mediate interactions between cells and interactions of cells with underlying matrix components [2; 62]. In the central nervous system (CNS), thrombospondin-4 (TSP4) is secreted primarily by astrocytes and promotes synaptogenesis [12; 39; 62]. Recently, TSP4 has been found to contribute to neuropathic pain pathogenesis [39]. TSP4 gene expression is elevated in DRGs after peripheral nerve injury [38], and intrathecal administration of TSP4 protein amplifies excitatory synaptic transmission in the spinal cord dorsal horn and produces mechanical and thermal sensitization that can be eliminated by antisense oligodeoxynucleotides, intrathecal antibodies, and TSP4 gene knockout [39]. Additionally, we have found increased TSP4 protein level in DRGs after peripheral nerve injury [56]. While these observations suggest a role for TSP4 in neuropathic pain, the specific actions of TSP4 in healthy and injured sensory neurons are unknown.

VGCCs are composed of a pore-forming α_1 subunit as well as auxiliary β , $\alpha_2\delta$ and γ subunits [10]. The $\alpha_2\delta$ subunits enhance I_{Ca} by modulating calcium channel trafficking and kinetics, and have been identified as the binding receptor of TSP4 [22]. Gabapentin (GBP), another $\alpha_2\delta_1$ ligand that is used in the management of neuropathic pain, blocks TSP-induced formation of excitatory synapses [16; 22], and reduces I_{Ca} after chronic administration [7; 31; 71]. Like TSP4, $\alpha_2\delta_1$ is upregulated after nerve injury in the involved DRGs [72], and $\alpha_2\delta_1$ knockout delays the onset of mechanical hypersensitivity after nerve injury [58]. Therefore, it is possible that TSP4 may act on VGCCs through binding to the $\alpha_2\delta_1$ subunit and thereby reduce I_{Ca} . To address this hypothesis, we first examined the effects of TSP4 on I_{Ca} through HVA and LVA calcium channels. As a further step, we additionally examined whether GBP pre-treatment can block the effects of TSP4 on HVA and LVA VGCCs.

2. Methods

2.1. Animals

All animal experiments were performed according to protocols approved by the Institutional Animal Care and Use Committee of the Medical College of Wisconsin (AUA00001809). Those animals were maintained and used according to the NIH *Guide for the Care and Use of Laboratory Animals*, and in compliance with federal, state, and local laws. DRGs from mice (8–12 weeks old) were rapidly harvested following deep isoflurane (2%) anesthesia and decapitation. *TSP4* wild-type (WT) and gene knock-out (KO) mice (B6.129P2-*Thbs4tm1Dgen/J*) were obtained from The Jackson Laboratory (Bar Harbor, Maine). These mice were bred internally, and adult male mice were used for most of the experiments and female mice were used to confirm major findings. All the genetically modified mice appeared normal with respect to grooming, social interactions, and feeding, and showed no signs of abnormality or any obvious motor defects, tremor, seizure, or ataxia. All animals were housed in a room with a 12/12 h day/night cycle and free access to food and water.

2.2. Neuron isolation and plating

After DRGs harvesting, ganglia were placed in a 35 mm dish containing $\text{Ca}^{2+}/\text{Mg}^{2+}$ -free, cold HBBS (Thermo Fisher Scientific, Waltham, MA) and cut into four to six pieces that were incubated in 0.01% blendzyme 2 (Roche Diagnostics, Indianapolis, IN) for 26 min followed by incubation in 0.25% trypsin (Sigma Aldrich, St. Louis, MO) and 0.125% DNase (Sigma) for 30 min, both dissolved in Dulbecco's modified Eagle's medium (DMEM)/F12 with glutaMAX (Invitrogen, Carlsbad, CA). After exposure to 0.1% trypsin inhibitor and centrifugation, the pellet was gently triturated in culture medium containing Neural Basal Media A with B27 supplement (Invitrogen), 0.5 mM glutamine, 10 ng/ml nerve growth factor 7S (Alomone Labs, Jerusalem, Israel) and 0.02 mg/ml gentamicin (Invitrogen). Dissociated neurons were plated onto poly-L-lysine coated glass cover slips (Deutsches Spiegelglas, Carolina Biological Supply, Burlington, NC) and maintained at 37°C in humidified 95% air and 5% CO_2 for 2 hours, and were studied no later than 8 hours after harvest.

2.3. Electrophysiological recording

Modified Tyrode's solution consists of the following (in mM): 140 NaCl, 4 KCl, 2 CaCl_2 , 2 MgCl_2 , 10 D-glucose, 10 HEPES at pH of 7.4 with NaOH and an osmolarity of 300 mOsm. Voltage-induced currents flowing through Ca^{2+} channels were recorded using an extracellular solution containing (in mM): 2 BaCl_2 , 4-aminopyridine 1, 10 HEPES, 140 tetraethylammonium chloride (TEACl), pH of 7.4, with an osmolarity of 300 mOsm. To record HVA I_{Ca} , the internal pipette solution contained (in mM): 110 Cs-methylsulfate, 10 TEA-Cl, 1 CaCl_2 , 1 MgCl_2 , 10 EGTA, 10 HEPES, 4 Mg-ATP, 0.3 Li_2 -GTP, at pH of 7.2 with CsOH and osmolarity of 296 to 300 mOsm. To selectively record LVA currents, neurons were preincubated in a Tyrode's solution with 0.2 μM ω -conotoxin GVIA, 0.2 μM nisoldipine and 0.2 μM ω -conotoxin MVIIC for at least 30 min. ω -conotoxin GVIA irreversibly blocks N-type calcium channels, and ω -conotoxin MVIIC irreversibly blocks P-/Q-type calcium channels. The concentrations used were saturating in preliminary experiments. Any residual HVA I_{Ca} following incubation of HVA calcium channel blockers

was eliminated by using fluoride in the internal pipette solution, which runs down HVA without reducing LVA I_{Ca} [52]. The fluoride (F⁻)-based internal solution, which was used in all experiments examining LVA currents, contained (in mM): 135 tetra-methyl ammonium hydroxide (TMA-OH), 10 EGTA, 40 HEPES, and 2 MgCl₂, adjusted to pH 7.2 with hydrofluoric acid (HF). A newly developed T-type Ca²⁺ channel blocker, TTA-P2, was used to confirm the T-type I_{Ca} [11]. Patch pipettes, ranging from 2–4MΩ resistance, were formed from borosilicate glass (King Precision Glass Co., Claremont, CA) and fire polished. Recordings were made with an Axopatch 700B amplifier (Molecular Devices, Downingtown, PA). Signals were filtered at 2 kHz and sampled at 10 kHz with a Digidata 1440A digitizer and pClamp10 software (Molecular Devices). Series resistance (5–10MΩ) was monitored before and after the recordings, and data were discarded if the resistance changed by 20%. After forming the whole cell recording, capacitance and series resistance were compensated accordingly. Leak currents were digitally subtracted using a P/4 leak subtraction protocol.

Voltage protocols consisted of 100-ms square-wave commands from a holding potential of –60 mV for HVA, or 400-ms square-wave commands from a holding potential of –90mV for LVA to +50 mV, in 10-mV increments with 5-s intervals between steps. Measured inward current was normalized by membrane capacitance, which results in a current density corrected for cell size (pA/pF). To determine the current-voltage (I–V) relationship of voltage-dependent activation, the peak current densities during each voltage command step were fitted to a smooth curve with a Boltzmann equation: $I = G_{max}(V - E_{rev}) / \{1 + \exp[(V - V_{1/2})/k]\}$, which provided the maximum conductance (G_{max}), the voltage at which current is half maximal ($V_{1/2}$), the reversal potential (E_{rev}) and the slope factor (k) that describes the voltage dependence of conductance. Steady-state inactivation was obtained with voltage protocols consisting of 4-s square-wave commands from a holding potential of –60 mV (for HVA) to +50 in increments of 10mV followed by 50ms at 0mV during which the peak current was recorded, or 1-s square-wave commands from a holding potential of –90mV (for LVA) to +20 mV in increments of 10mV followed by 50ms at –10mV for recording. The current densities for each voltage command (I–V) were analyzed with an equation: $I/I_{max} = 1 / \{1 + \exp[(V - V_{1/2})/k]\}$, where I is the current, V is the voltage command, I_{max} is the maximum current, $V_{1/2}$ is the voltage at which current is half-maximal, k is a slope factor describing voltage dependence of conductance.

Sensory neuron somatic diameter is broadly associated with specific sensory modalities. We therefore stratified neurons as large (>27 μm), which represent predominantly fast conducting non-nociceptive neurons, or small (< 27 μm), which represent predominantly nociceptive neurons. Unless otherwise stated, small neurons were examined. Small neurons were further characterized by binding of isolectin B4 (IB4) labeled with fluorescein isothiocyanate (Sigma-Aldrich, St. Louis, MO; 10 μg/mL, 10 min) and considered IB4-positive when they stained with a complete ring around the neuronal profile. This is an established method of grouping mouse sensory neurons [5].

2.4. Measurement of cytoplasmic Ca²⁺ concentration

Measurement of cytoplasmic Ca²⁺ concentration ($[Ca^{2+}]_c$) was performed following our previously published protocols [21; 28]. Unless otherwise specified, regular Tyrode's solution was used to bathe the neurons. Stock solution of Fura-2-AM (Invitrogen) was dissolved in DMSO, and subsequently diluted in the relevant bath solution such that the final bath concentration of DMSO was 0.2% or less, which does not affect $[Ca^{2+}]_c$ [27]. The 500 μ l recording chamber was superfused by gravity-driven flow at a rate of 3 ml/min. Agents were delivered by directed microperfusion controlled by a computerized valve system through a 500 μ m diameter hollow quartz fiber 300 μ m upstream from the neurons. This flow completely displaced the bath solution, and constant flow was maintained through this microperfusion pathway by delivery of bath solution when specific agents were not being administered. Dye imaging has shown that solution changes are achieved within 200 ms.

Neurons plated on cover slips were exposed to Fura-2-AM (5 μ M) at room temperature in a solution that contained 2% bovine albumin to aid dispersion of the fluorophore. After 30 min, they were washed 3 times with regular Tyrode's solution, given 30 minutes for de-esterification, and then mounted in the recording chamber. Neurons were first examined under bright field illumination, and those showing signs of lysis, crenulation or superimposed glial cells were excluded. For $[Ca^{2+}]_c$ recording, the fluorophore was excited alternately with 340 nm and 380 nm wavelength illumination (150 W Xenon, Lambda DG-4, Sutter, Novato, CA), and images were acquired at 510 nm using a cooled 12-bit digital camera (Coolsnapfx, Photometrics, Tucson, AZ) and inverted microscope (Diaphot 200, Nikon Instruments, Melville, NY) through a 20X objective. Recordings from each neuron were obtained as separate regions (MetaFluor, Molecular Devices) at a rate of 3 Hz. After background subtraction, the fluorescence ratio R for individual neurons was determined as the intensity of emission during 340 nm excitation (I_{340}) divided by I_{380} , on a pixel-by-pixel basis. The Ca²⁺ concentration was then estimated by the formula $K_d \cdot \beta \cdot (R - R_{min}) / (R_{max} - R)$ where $\beta = (I_{380max}) / (I_{380min})$. Values of R_{min} , R_{max} and β were determined by in-situ calibration and were 0.38, 8.49 and 9.54, and K_d was 224 nm. Only neurons with stable baseline R traces were further evaluated. Traces were analyzed using Axograph X 1.1 (Axograph Scientific, Sydney, Australia). Transient changes in $[Ca^{2+}]_c$ were generated by depolarization produced by microperfusion application of K⁺ (50 mM) for 0.3 s or 1 s.

2.5. Injury model preparation and Sensory testing

Twenty one mice were subjected to SNL, based on the original technique [40] with modifications [28; 61]. Briefly, during anesthesia by inhalation of isoflurane, the right lumbar paravertebral region was exposed through a midline incision, and the fifth lumbar (L5) transverse process was removed to expose the L4 spinal nerve, which was ligated with 6-0 silk suture and severed approximately 1 mm distal to their respective DRGs. The wounds were closed in layers and the skin stapled. Control mice received sham surgery in the form of skin incision and closure only.

Sensory behavior was evaluated before and after surgery by observing induced responses to a noxious mechanical stimulus. Briefly, on three different days between 10 and 17 days after surgery, the right plantar skin was touched (10 stimuli/test, stimuli repeated within 5s of

replacing the foot on the cage floor) with a 22-G spinal needle with adequate pressure to indent but not penetrate the skin. Whereas control animals respond with only a brief reflexive withdrawal, mice following SNL may display a complex hyperalgesia response that includes licking, chewing, grooming and sustained elevation of the paw. The average frequency of hyperalgesia responses over the 3 testing days was tabulated for each mouse. We have previously confirmed that this method is a valid representation of pain using conditioned place avoidance [75]. After SNL, only mice that displayed a hyperalgesia-type response after at least 20% of stimuli were used further in this study.

2.6. Reagents

ω -conotoxin GVIA, ω -conotoxin MVIIC, nisoldipine, and all other common chemicals were obtained from Sigma-Aldrich. TTA-P2 was provided by Merck and Co., Inc. TSP4 proteins were extracted and purified according to our previous report [39].

2.7. Statistical analysis

Statistical analyses were performed with Clampfit (Molecular Devices), Graphpad Prism 6 (GraphPad Software, Inc, CA) and Sigmaplot11.0 (Systat Software Inc, Chicago, IL). Student's t-test, one-way, two-way or two-way repeated measures ANOVA with Tukey's *post hoc* analysis were used to test significance of differences between groups. When planned comparisons were performed by t-test between more than two groups, familywise error was controlled by Bonferroni correction. A *P* value less than 0.05 was considered significant. Data are reported as mean \pm SEM. The IC_{50} of the concentration-response curve was determined with a Langmuir function: $Y = Y_{min} + (Y_{max} - Y_{min}) / (1 + 10^{(X - \log IC_{50})})$, where *Y* is the response, Y_{max} and Y_{min} are maximal and minimal effects respectively, *X* is the TSP4's concentration used, and IC_{50} is the effective concentration of TSP4 for 50% response.

3. Results

3.1. TSP4 inhibits HVA VGCCs in DRG neurons

To record HVA currents, all neurons were clamped at -60 mV and depolarized with a series of 100 ms square wave protocol with voltage commands from -60 mV to 60 mV in 10 mV increments (Fig. 1A). HVA currents were present in all neurons and showed an activation threshold of between -30 and -20 mV and peak between -10 and 0 mV. It had been shown that TSP4 expression is increased after painful nerve injury [39; 56], while I_{Ca} and resting $[Ca^{2+}]_c$ are decreased in sensory neurons of rats following nerve injury [25; 53]. We therefore asked whether increased expression of TSP4 can cause decreased I_{Ca} . We found that bath application of TSP4 for 20 minutes did not significantly inhibit HVA I_{Ca} (Fig. 1B). Since increased spinal TSP4 induces dorsal horn neuron sensitization and behavioral hypersensitivity through a chronic, but not acute, mechanism [39], we tested the effect of sustained TSP4 application on HVA I_{Ca} . Incubation of TSP4 for 4 hours produced significant inhibition on HVA I_{Ca} in DRG neurons prepared from naive mice (Fig. 1C, D). This inhibition was concentration-dependent (Fig. 1D). Fitting the concentration-response data with a Langmuir function yielded a value for half-maximal inhibition (IC_{50}) of 15.1 ± 1.2 nM (Fig. 1D). TSP4 inhibited HVA I_{Ca} in DRG neurons of all sizes (Fig. 1E, F).

Denatured TSP4 had no effect on peak HVA I_{Ca} (106.1 ± 11.6 pA/pF, $n = 5$, $P = 0.05$ compared with vehicle control). TSP4 had similar effects on HVA I_{Ca} in DRG neurons from female mice (Control: 103.7 ± 8.9 pA/pF, $n = 6$; TSP4 treatment: Control: 43.3 ± 4.8 pA/pF, $n = 7$; $P < 0.01$).

Ligands can cause conformational changes in an ion channel that modulate functional properties like activation and inactivation. Since functional properties of Ca^{2+} channels are affected by peripheral nerve injury [54], we examined the action of TSP4 on voltage dependence and kinetics of HVA I_{Ca} . TSP4 application did not alter the voltage dependence of activation (Fig. 2A). TSP4 treatment substantially reduced G_{max} but did not change $V_{1/2}$ and k (Fig. 2A). Steady state inactivation was shifted to the right after TSP4 treatment (Fig. 2B), such that the availability of HVA I_{Ca} after a preceding depolarization pulse was somewhat higher in cells treated with TSP4. The I_{Ca} traces during depolarization to -10 mV from a holding potential of -100 mV were fit to a single exponential to characterize the effect of TSP4 on HVA I_{Ca} inactivation kinetics, which showed that average inactivation rates were significantly faster for TSP4 treatment compared to vehicle control (Fig. 2C). The ratio of current persisting after 2s of depolarization normalized against the initial peak was also used to characterize the effect of TSP4 on HVA I_{Ca} inactivation kinetics, which revealed greater inactivation during depolarizations to both -10 and 0 mV (Fig. 2C). Taken together, the effect of TSP4 on HVA I_{Ca} is to reduce initial peak current and to accelerate current inactivation.

3.2. TSP4 reduces I_{Ca} conducted by N- and L-type calcium channels

N- and L-type channels conduct the majority of inward Ca^{2+} flux in most DRG neurons and they contribute to sensory neuron dysfunction and pain after nerve injury [54]. We therefore hypothesized that N- and L-type calcium channels would be most affected by TSP4 treatment. Because of the uncertainties produced by combined application of multiple VGCCs blockers, we examined N-type or L-type currents by determining sensitivity of I_{Ca} to TSP4 in neurons in which N- or L-type current has been selectively eliminated by the application of ω -conotoxin GVIA or nisoldipine without other antagonists [54] (Fig. 3A, B). During blockade of N-type I_{Ca} by application of ω -conotoxin GVIA, TSP4 still reduced residual HVA I_{Ca} (Fig. 3A, D). During blockade of L-type HVA I_{Ca} , TSP4 likewise reduced residual HVA I_{Ca} (Fig. 3B, D). It is reported that P/Q- type VGCCs are expressed at pre-synaptic terminals in the spinal dorsal horn and play a role in pain processing [57]. To test effects of TSP4 on P/Q- type VGCCs, we isolated P/Q- type VGCCs by blockade of N-type current (ω -conotoxin GVIA, 200 nM), L-type (Nisoldipine, 5 μ M), most of R-type (SNX-482, 200 nM), and T-type (TTA-P2, 500 nM). TSP4 did not reduce the residual P/Q- type I_{Ca} (Fig. 3C, D). Taken together, these data indicate that most of the reduced total I_{Ca} lost with TSP4 application is from reduction of N- and L-type I_{Ca} .

3.3. TSP4 increases I_{Ca} conducted by T-type calcium channels

LVA VGCCs critically regulate the excitability of many neural systems and may participate in enhancing neural activity in nociceptive pathways [69]. Neurons dissociated from rats with neuropathic pain following peripheral injury have showed upregulated LVA I_{Ca} in small DRG neurons [35]. We asked whether TSP4 has the same inhibitory effects on LVA

channels as we had so far found for HVA channels. LVA current was isolated by blocking HVA currents with specific toxins (see Methods). Neurons were initially tested by depolarization from a holding potential of -60mV to a test potential of -40mV during which a minority (vehicle control: 8 of 61, 11.2%; TSP4: 9 of 56, 13.8%) showed distinctive large LVA currents greater than 10pA/pF , which are typical of low-threshold mechanoreceptor or D-hair receptor neurons [20; 45; 64]. These D-hair neurons were excluded from further analysis. LVA I_{Ca} in the other neurons, which was measured by depolarizations from a holding potential of -90mV , peaked at negative potentials (from -10 to -20mV) (Fig. 4A,B). The identity of this current as T-type was confirmed by blockade with the selective T-type Ca^{2+} channel blocker TTA-P2 (Fig. 4C).

Interestingly, sustained TSP4 exposure caused increased peak LVA I_{Ca} (Fig. 4A,B) in DRG neurons of all sizes (Fig. 4D,E). Denatured TSP4 had no effect on peak LVA I_{Ca} ($29 \pm 3.5\text{ pA/pF}$, $n = 5$, $P = 0.52$ compared with vehicle control). DRG neurons from female mice showed similar TSP4 effects on LVA I_{Ca} (Control: $20.9 \pm 2.6\text{ pA/pF}$, $n = 6$; TSP4 treatment: $42.2 \pm 3.8\text{ pA/pF}$, $n = 7$; $P < 0.01$). TSP4 treatment did not change kinetics of voltage dependence of activation (Fig. 5A), or voltage dependence of steady state inactivation (Fig. 5B). TSP4 accelerated both of the fast and slow components of current inactivation during persistent depolarization (Fig. 5C). Despite the accelerated inactivation caused by TSP4, total charge transfer during depolarization was nonetheless greater in TSP4-treated neurons, and averaged LVA current density remained greater in TSP4-treated neurons throughout the duration of depolarization (Fig. 5C), which could contribute to repetitive AP firing. TSP4 treatment caused slower deactivation kinetics (Fig. 5D), which could further elevate total charge transfer. TSP4 delayed the recovery of inactivated LVA I_{Ca} , normalized to the initial peak LVA current (Fig. 5E). However, additional analysis shows that current density (pA/pF) in TSP4-treated neurons is nonetheless greater than vehicle controls at all time points during recovery (Fig. 5E). Taken together, these observations support the view that the net effect of TSP4 is to elevate LVA current during and following depolarization.

3.4. TSP4 decreases $[\text{Ca}^{2+}]_{\text{c}}$ via HVA and increases $[\text{Ca}^{2+}]_{\text{c}}$ via LVA

Intracellular Ca^{2+} levels ($[\text{Ca}^{2+}]_{\text{c}}$) regulate critical neuronal functions such as excitation, release of neurotransmitters, and differentiation, and dysregulation of $[\text{Ca}^{2+}]_{\text{c}}$ signaling leads to diverse neuropathological conditions [23; 29]. Upon neuronal activation, Ca^{2+} entering through VGCCs is buffered, sequestered, and ultimately extruded from the neuron to maintain Ca^{2+} homeostasis. Our prior findings show that painful peripheral nerve injury leads to aberrant Ca^{2+} signaling in peripheral sensory neurons, including lower resting $[\text{Ca}^{2+}]_{\text{c}}$ [25] and reduced activity-induced cytoplasmic Ca^{2+} transients [26]. We therefore examined the possibility that TSP4 regulates these features. TSP4 4 hr incubation did not affect resting $[\text{Ca}^{2+}]_{\text{c}}$ (Control: $114.0 \pm 5.3\text{ nM}$, $n = 76$; TSP4: $103.9 \pm 3.4\text{ nM}$, $n = 111$; $P = 0.094$ by Student's *t*-test). To test activity-induced changes in $[\text{Ca}^{2+}]_{\text{c}}$, we depolarized sensory neurons by exposure to 50 mM K^{+} for either 1s or 0.3s, to model graded depolarizations (Fig. 6A). Specifically, 1s administration of K^{+} depolarized neurons to 0mV , and initiated Ca^{2+} transients that were only partially sensitive to blockade by the selective T-type Ca^{2+} channel blocker TTA-P2 (Control: $2068.3 \pm 260.4\text{ nM}$, $n = 8$; TTA-P2: $1561.6 \pm 239.0\text{ nM}$, $n = 8$; $P = 0.174$ by Student's *t*-test, Fig. 6B.). In contrast, 0.3s application of

K⁺ depolarized neurons to only -30mV, which produced transients that were eliminated by TTA-P2 (Control: 532.6 ± 55.4 nM, n = 10; TTA-P2: 149.7 ± 67.4 nM, n = 10; $P < 0.001$ by Student's t-test, Fig. 6B). Using these two different models of depolarization, we found diverging regulation of [Ca²⁺]_c by TSP4 that depended on the manner of depolarization. Specifically, whereas TSP4 diminished transients induced by sustained, full depolarization (Fig. 6C), transients activated by partial depolarization were amplified (Fig. 6D). These findings demonstrate that TSP4 modulation of neuronal function depends upon the extent to which the neuron is depolarized, due to selective inhibition of HVA vs. activation of LVA channels.

3.5. TSP4 regulates HVA and LVA through the $\alpha_2\delta_1$ calcium subunit

It has been shown that the VGCC $\alpha_2\delta_1$ subunit is the binding site of TSP4 [22], which suggests that TSP4 inhibits HVA I_{Ca} and increases LVA I_{Ca} through actions on the $\alpha_2\delta_1$ subunit. To test this idea, we examined whether GBP, a drug that relieves neuropathic pain by binding to the $\alpha_2\delta_1$ subunit [31], can block TSP4's effects on VGCCs. Application of GBP, using a concentration (25 μ M) previously shown to reach maximum effects on HVA I_{Ca} in DRG neurons [67], had no direct effects on VGCCs when applied either acutely (data not shown) or by incubation for 4 hours (Fig. 7A), as we have shown previously [44]. However, GBP blocked TSP4's effects on both HVA and LVA I_{Ca} (Fig. 7A). GBP likewise eliminated TSP4's regulation of activation-induced [Ca²⁺]_c transients during both sustained, full depolarization as well as brief, partial depolarization (Fig. 7B). Taken together, these data suggest that TSP4 acts on VGCCs by specifically targeting the $\alpha_2\delta_1$ calcium subunit.

3.6. TSP4 is required to mediate the effect of nerve injury on HVA and LVA I_{Ca}

Nerve injury disrupts Ca²⁺ signaling in DRG neurons. The findings noted above make it possible that altered I_{Ca} in injured sensory neurons results from up-regulated TSP4 *in vivo*. This is also supported by the lack of pain behavior after SNL in mice that lack TSP4 [39]. To probe this question further, we used TSP4 KO mice, compared to their WT littermates, to determine if TSP4 expression is necessary to mediate the effects of injury on sensory neuron I_{Ca}. In the WT control mice, injury by SNL produced the expected loss of HVA I_{Ca} after injury as demonstrated by I-V curves and peak I_{Ca} (Fig. 8A,B). Uninjured neurons from TSP4 KO mice had currents that did not differ from WT mice, but the injury effect on HVA I_{Ca} was eliminated in these neurons lacking TSP4 (Fig. 8A,B). Neurons from WT mice also developed the expected elevation of LVA I_{Ca} following injury (Fig. 8C,D). However, neurons from TSP4 KO mice failed to show an injury effect on LVA I_{Ca} (Fig. 8C,D). These findings indicate that injury-induced down-regulation of HVA and up-regulation of LVA I_{Ca} are dependent on newly synthesized TSP4.

Since elevated TSP4 after nerve injury may in part account for decreased HVA and increased LVA, it can be expected that the subsequent effects of TSP4 application would be occluded. We found that the regulation of HVA and LVA by TSP4 previously identified in uninjured mice (Fig. 1,4) was eliminated in DRG neurons from SNL mice (Fig. 9), consistent with the interpretation that injury-induced elevation of TSP4 within the DRG precludes the effect of experimentally applied TSP4 [56]. Lack of sensitivity of injured neurons to applied TSP4 adds further support to the view that TSP4 mediates the effect of injury on I_{Ca}.

4. Discussion

This study was designed to identify the regulation of sensory neuron VGCCs by TSP4. We first found that TSP4 reduces HVA I_{Ca} in a concentration-dependent fashion, and it reduces current through the dominant N- and L- channel subtypes. In contrast, TSP4 increases LVA I_{Ca} . These actions on VGCCs require the participation of the $\alpha_2\delta_1$ calcium channel subunit, and are sensitive to GBP, another ligand of the $\alpha_2\delta_1$ calcium channel subunit. Our observation of similar levels of I_{Ca} in WT and TSP4 KO animals suggests that TSP4 levels in the uninjured state are very low, but we have previously found that painful nerve injury increases gene expression and protein levels of TSP4 in the DRG [38; 56]. Additional support for a possible TSP4 pathogenic role in causing pain after nerve injury comes from observations that intrathecal TSP4 application generates pain and that TSP4 KO mice don't develop hyperalgesia after nerve injury [39].

Prior studies by us as well as by others demonstrate decreased HVA I_{Ca} and in sensory neurons after peripheral nerve injury [1; 3; 25; 26; 53; 54]. We now report that TSP4 reduces HVA I_{Ca} and also diminishes $[Ca^{2+}]_c$ elevation following VGCC activation by full, sustained depolarization. We can therefore identify TSP4 as a potential link between nerve injury and I_{Ca} loss in sensory neurons. Several previously described mechanisms have been proposed for post-injury loss of I_{Ca} . For instance, I_{Ca} through N-type channels can be modulated by glial-derived neurotrophic factor activation of extracellular signal-regulated kinase (ERK) [13; 51; 73]. Other kinases such as protein kinase C and CaMKII regulate both L- and N-type VGCCs [34; 42; 68; 77], and we have found diminished levels of phosphorylated CaMKII following sensory neuron injury [4; 37; 41]. Thus, TSP4's effects on VGCCs could involve signaling through these kinase pathways. Additionally, since $\alpha_2\delta$ subunits substantially delay internalization and degradation of VGCCs [6], disruption of $\alpha_2\delta$ function by TSP4 may allow rapid removal of functional Ca^{2+} channels from the plasma membrane.

Loss of HVA current contributes to increased excitability of DRG neurons and has important implications for pain processing. In the dorsal horn, blockade of HVA Ca^{2+} channels can produce analgesia through interruption of synaptic transmission [9], although the net effect of synaptic inhibition will depend on the balance of effects on dorsal horn excitatory vs. inhibitory pathways [70]. In contrast, at the level of the sensory neuron, intracellular Ca^{2+} activates $I_{K(Ca)}$ and thereby limits membrane excitability [32; 46], which in turn regulates repetitive neuronal firing and propagation of impulse trains [28; 68]. Therefore, although the actions of TSP4 on HVA channels in the dorsal horn could be expected to reduce pain, TSP4-induced loss of I_{Ca} in the peripheral portion of the sensory neuron could enhance generation and transmission of AP trains, which is recognized as an important etiologic factor in neuropathic pain [60]. This latter role for TSP4 is supported by recognition that elevated sensory neuron excitability is a key contributor to generation of neuropathic pain following nerve injury [15; 63; 74]. Further support for considering TSP4 as a critical pain-generating molecule is provided by the delayed and diminished hyperalgesia that evolves after nerve injury in animals lacking the $\alpha_2\delta_1$ subunit [58], which is the principal receptor for TSP4.

Peripheral nerve injury and inflammation result in a marked upregulation of the $\alpha_2\delta_1$ subunit in sensory neurons of the DRG [44; 47; 48]. Transgenic $\alpha_2\delta_1$ overexpression produces enhanced I_{Ca} in sensory neurons, as well as accelerated channel opening and depolarized voltage dependence of channel activation [44], while chronic lack of $\alpha_2\delta_1$ or application of GBP decreases HVA channel trafficking to the neuronal membrane [31]. Thus, $\alpha_2\delta_1$ overexpression after peripheral nerve injury should increase I_{Ca} , yet the opposite is found, as noted above. Our new data showing that TSP4 reduces I_{Ca} through HVA channels resolves this paradox. Specifically, we speculate that elevated levels of TSP4 account for decreased HVA I_{Ca} through dominant actions on membrane-resident channels in an $\alpha_2\delta_1$ -dependent fashion. By binding to the upregulated $\alpha_2\delta_1$ subunits, injury-induced TSP4 alters channel function or number to dramatically reduce I_{Ca} .

In addition to HVA channels, elevated LVA I_{Ca} in primary afferent neurons have also been implicated in pain generation after peripheral nerve injury [35], related to the excitatory influence of T-type channel opening during weak depolarization. Our present data show that application of TSP4 to putative nociceptive sensory neurons increases LVA I_{Ca} . This result, combined with observations that T-type calcium channels support repetitive firing of DRG neurons [36; 55], provides a second mechanism whereby elevated TSP4 after nerve injury may make sensory neurons hyperexcitable. Although we have previously observed an absence of medium-sized neurons with large LVA current typical of D-hair type neurons after nerve injury [52], those neurons were excluded in the present study. Other studies have demonstrated injury-induced amplification of LVA current in the broad population of sensory neurons [35]. This sensitivity of LVA I_{Ca} to TSP4 implies a role of the $\alpha_2\delta_1$ subunit in regulating LVA I_{Ca} , which was confirmed by our blockade of the TSP4 suppression of LVA I_{Ca} by co-administration of GBP. Unlike HVA channels, a clear role for auxiliary subunits in the expression of LVA channels has not been established [16], although evidence has shown that LVA I_{Ca} is increased by co-expression with $\alpha_2\delta_1$ subunit, and that membrane trafficking of expressed LVA channels is enhanced by the $\alpha_2\delta_1$ subunit [17; 19; 76]. Our findings provide further evidence of a role for $\alpha_2\delta_1$ in regulating LVA I_{Ca} in sensory neurons.

Considering that the $\alpha_2\delta_1$ subunit directly interacts with HVA VGCCs but not with LVA VGCCs, it seems paradoxical that TSP4 binding with the $\alpha_2\delta_1$ subunit causes bidirectional effects on HVA I_{Ca} and LVA I_{Ca} . It is possible, however, that a component of the effects of TSP4 on HVA and LVA could be through actions on intracellular signaling pathways. Ligand binding to the $\alpha_2\delta_1$ subunit has been shown to suppress intracellular signaling pathways including PKC, c-Raf, ERK1/2, and ELK-1 [8; 30]. These in turn could influence HVA and LVA function differently. For instance, in fibroblasts, activation of MEK/ERK pathway inhibits LVA VGCCs [66], so its loss would result in elevated LVA function. In sensory neurons, blockade of MEK/ERK pathway can decrease N-type VGCCs [51], replicating our finding with TSP4 application. Further study of potential $\alpha_2\delta_1$ subunit-induced signaling will be needed.

Our findings additionally cast new light on the analgesic mechanism of GBP. The regulation of VGCCs by GBP has previously been examined without consideration of the role of TSP4. This may explain observations that GBP regulation of I_{Ca} may depend on culture conditions

[50] and induced disease states [49] and that effects on I_{Ca} are generally small and inconsistent between studies [14]. While it is clear that the analgesic efficacy of GBP for pain following nerve injury requires binding to the $\alpha_2\delta_1$ subunit [24] and that GBP reduces the trafficking of VGCCs to the neuronal membrane [31], our new data suggest that a contributing analgesic effect of GBP may be via interrupting the action of TSP4 upon $\alpha_2\delta_1$ subunit, the main binding partner of both. It has been noted that GBP is most effective in sensitized pain states, but is less effective against normal nociception [18], consistent with a mechanism targeting TSP4. Furthermore, although GBP can suppress I_{Ca} directly, this requires a concentration at the level of 1mM and a duration of 3 days [31], whereas our data show that GBP is effective in blocking the action of TSP4 upon I_{Ca} at a concentration of 25 μ M within 4 hours. Thus, under conditions that resemble the environment of the sensory neuron after peripheral nerve injury, GBP has clear effects on I_{Ca} [44]. By competitively binding the $\alpha_2\delta_1$ subunit, GBP prevents the actions of TSP4 on VGCCs, so it is possible that a substantial component of the therapeutic benefit of GBP is through blocking TSP4's suppression of HVA I_{Ca} and amplification of LVA I_{Ca} . While TSP4-induced loss of I_{Ca} is excitatory in peripheral portions of the sensory neuron, decreased I_{Ca} in presynaptic sites in the dorsal horn would lead to less release of excitatory neurotransmitters. This suggests that either actions of GBP at peripheral sites predominantly account for GBP analgesia, or that effects in the dorsal horn other than regulation of I_{Ca} produce analgesia. It is known that TSP4 is synaptogenic and that GBP can block this effect [22], while other findings show 4 days application of TSP4, but not acute application, results in elevated excitatory synaptic transmission in the dorsal horn [39]. These findings together suggest that regulation of TSP4-induced synaptogenesis may be a prominent mechanism contributing to GBP analgesia.

In summary, our results add support to the view that TSP4 may be an important pain mediator. Prior research has established TSP4 as a critical element in triggering excitatory synapse formation through binding the $\alpha_2\delta_1$ subunit [22], which may be a mechanism for inducing chronic pain. Our findings now implicate TSP4 as a possibly important pathogenic influence on HVA and LVA VGCCs. By addressing these injury-induced mechanisms, control of TSP4 signaling may be a particularly promising approach for treating neuropathic pain.

Acknowledgments

The study was supported by National Institutes of Health Grant R01DE021847 (to Z.D.L. & Q.H. H.). TTA-P2 was kindly provided by Merck and Co., Inc.

References

1. Abdulla FA, Smith PA. Axotomy- and autotomy-induced changes in Ca^{2+} and K^{+} channel currents of rat dorsal root ganglion neurons. *J Neurophysiol.* 2001; 85(2):644–658. [PubMed: 11160500]
2. Adams JC. Thrombospondins: multifunctional regulators of cell interactions. *Annu Rev Cell Dev Biol.* 2001; 17:25–51. [PubMed: 11687483]
3. Baccei ML, Kocsis JD. Voltage-gated calcium currents in axotomized adult rat cutaneous afferent neurons. *J Neurophysiol.* 2000; 83(4):2227–2238. [PubMed: 10758131]

4. Bangaru ML, Meng J, Kaiser DJ, Yu H, Fischer G, Hogan QH, Hudmon A. Differential expression of CaMKII isoforms and overall kinase activity in rat dorsal root ganglia after injury. *Neuroscience*. 2015; 300:116–127. [PubMed: 25982557]
5. Barabas ME, Kossyрева EA, Stucky CL. TRPA1 is functionally expressed primarily by IB4-binding, non-peptidergic mouse and rat sensory neurons. *PLoS One*. 2012; 7(10):e47988. [PubMed: 23133534]
6. Bernstein GM, Jones OT. Kinetics of internalization and degradation of N-type voltage-gated calcium channels: role of the alpha2/delta subunit. *Cell Calcium*. 2007; 41(1):27–40. [PubMed: 16759698]
7. Biggs JE, Boakye PA, Ganesan N, Stemkowski PL, Lantero A, Ballanyi K, Smith PA. Analysis of the long-term actions of gabapentin and pregabalin in dorsal root ganglia and substantia gelatinosa. *J Neurophysiol*. 2014; 112(10):2398–2412. [PubMed: 25122705]
8. Boileau C, Martel-Pelletier J, Brunet J, Schrier D, Flory C, Boily M, Pelletier JP. PD-0200347, an alpha2delta ligand of the voltage gated calcium channel, inhibits in vivo activation of the Erk1/2 pathway in osteoarthritic chondrocytes: a PKCalpha dependent effect. *Ann Rheum Dis*. 2006; 65(5):573–580. [PubMed: 16249226]
9. Cao YQ. Voltage-gated calcium channels and pain. *Pain*. 2006; 126(1–3):5–9. [PubMed: 17084979]
10. Catterall WA. Structure and regulation of voltage-gated Ca²⁺ channels. *Annu Rev Cell Dev Biol*. 2000; 16:521–555. [PubMed: 11031246]
11. Choe W, Messinger RB, Leach E, Eckle VS, Obradovic A, Salajegheh R, Jevtovic-Todorovic V, Todorovic SM. TTA-P2 is a potent and selective blocker of T-type calcium channels in rat sensory neurons and a novel antinociceptive agent. *Mol Pharmacol*. 2011; 80(5):900–910. [PubMed: 21821734]
12. Christopherson KS, Ullian EM, Stokes CC, Mallowney CE, Hell JW, Agah A, Lawler J, Mosher DF, Bornstein P, Barres BA. Thrombospondins are astrocyte-secreted proteins that promote CNS synaptogenesis. *Cell*. 2005; 120(3):421–433. [PubMed: 15707899]
13. Dai Y, Iwata K, Fukuoka T, Kondo E, Tokunaga A, Yamanaka H, Tachibana T, Liu Y, Noguchi K. Phosphorylation of extracellular signal-regulated kinase in primary afferent neurons by noxious stimuli and its involvement in peripheral sensitization. *J Neurosci*. 2002; 22(17):7737–7745. [PubMed: 12196597]
14. Davies A, Hendrich J, Van Minh AT, Wratten J, Douglas L, Dolphin AC. Functional biology of the alpha(2)delta subunits of voltage-gated calcium channels. *Trends Pharmacol Sci*. 2007; 28(5):220–228. [PubMed: 17403543]
15. Djouhri L, Koutsikou S, Fang X, McMullan S, Lawson SN. Spontaneous pain, both neuropathic and inflammatory, is related to frequency of spontaneous firing in intact C-fiber nociceptors. *J Neurosci*. 2006; 26(4):1281–1292. [PubMed: 16436616]
16. Dolphin AC. The alpha2delta subunits of voltage-gated calcium channels. *Biochim Biophys Acta*. 2013; 1828(7):1541–1549. [PubMed: 23196350]
17. Dolphin AC, Wyatt CN, Richards J, Beattie RE, Craig P, Lee JH, Cribbs LL, Volsen SG, Perez-Reyes E. The effect of alpha2-delta and other accessory subunits on expression and properties of the calcium channel alpha1G. *J Physiol*. 1999; (519 Pt 1):35–45. [PubMed: 10432337]
18. Dooley DJ, Taylor CP, Donevan S, Feltner D. Ca²⁺ channel alpha2delta ligands: novel modulators of neurotransmission. *Trends Pharmacol Sci*. 2007; 28(2):75–82. [PubMed: 17222465]
19. Dubel SJ, Altier C, Chaumont S, Lory P, Bourinet E, Nargeot J. Plasma membrane expression of T-type calcium channel alpha(1) subunits is modulated by high voltage-activated auxiliary subunits. *J Biol Chem*. 2004; 279(28):29263–29269. [PubMed: 15123697]
20. Dubreuil AS, Boukhaddaoui H, Desmadryl G, Martinez-Salgado C, Moshourab R, Lewin GR, Carroll P, Valmier J, Scamps F. Role of T-type calcium current in identified D-hair mechanoreceptor neurons studied in vitro. *J Neurosci*. 2004; 24(39):8480–8484. [PubMed: 15456821]
21. Duncan C, Mueller S, Simon E, Renger JJ, Uebele VN, Hogan QH, Wu HE. Painful nerve injury decreases sarco-endoplasmic reticulum Ca(2)(+)-ATPase activity in axotomized sensory neurons. *Neuroscience*. 2013; 231:247–257. [PubMed: 23219911]

22. Eroglu C, Allen NJ, Susman MW, O'Rourke NA, Park CY, Ozkan E, Chakraborty C, Mulinyawe SB, Annis DS, Huberman AD, Green EM, Lawler J, Dolmetsch R, Garcia KC, Smith SJ, Luo ZD, Rosenthal A, Mosher DF, Barres BA. Gabapentin receptor alpha2delta-1 is a neuronal thrombospondin receptor responsible for excitatory CNS synaptogenesis. *Cell*. 2009; 139(2):380–392. [PubMed: 19818485]
23. Fernyhough P, Calcutt NA. Abnormal calcium homeostasis in peripheral neuropathies. *Cell Calcium*. 2010; 47(2):130–139. [PubMed: 20034667]
24. Field MJ, Cox PJ, Stott E, Melrose H, Offord J, Su TZ, Bramwell S, Corradini L, England S, Winks J, Kinloch RA, Hendrich J, Dolphin AC, Webb T, Williams D. Identification of the alpha2-delta-1 subunit of voltage-dependent calcium channels as a molecular target for pain mediating the analgesic actions of pregabalin. *Proc Natl Acad Sci U S A*. 2006; 103(46):17537–17542. [PubMed: 17088553]
25. Fuchs A, Lirk P, Stucky C, Abram SE, Hogan QH. Painful nerve injury decreases resting cytosolic calcium concentrations in sensory neurons of rats. *Anesthesiology*. 2005; 102(6):1217–1225. [PubMed: 15915036]
26. Fuchs A, Rigaud M, Hogan QH. Painful nerve injury shortens the intracellular Ca²⁺ signal in axotomized sensory neurons of rats. *Anesthesiology*. 2007; 107(1):106–116. [PubMed: 17585222]
27. Gemes G, Bangaru ML, Wu HE, Tang Q, Weihrauch D, Koopmeiners AS, Cruikshank JM, Kwok WM, Hogan QH. Store-operated Ca²⁺ entry in sensory neurons: functional role and the effect of painful nerve injury. *J Neurosci*. 2011; 31(10):3536–3549. [PubMed: 21389210]
28. Gemes G, Oyster KD, Pan B, Wu HE, Bangaru ML, Tang Q, Hogan QH. Painful nerve injury increases plasma membrane Ca²⁺-ATPase activity in axotomized sensory neurons. *Mol Pain*. 2012; 8:46. [PubMed: 22713297]
29. Gleichmann M, Mattson MP. Neuronal calcium homeostasis and dysregulation. *Antioxid Redox Signal*. 2011; 14(7):1261–1273. [PubMed: 20626318]
30. Gu Y, Huang LY. Gabapentin actions on N-methyl-D-aspartate receptor channels are protein kinase C-dependent. *Pain*. 2001; 93(1):85–92. [PubMed: 11406342]
31. Hendrich J, Van Minh AT, Heblich F, Nieto-Rostro M, Watschinger K, Striessnig J, Wratten J, Davies A, Dolphin AC. Pharmacological disruption of calcium channel trafficking by the alpha2delta ligand gabapentin. *Proc Natl Acad Sci U S A*. 2008; 105(9):3628–3633. [PubMed: 18299583]
32. Hogan Q, Lirk P, Poroli M, Rigaud M, Fuchs A, Phillip P, Ljubkovic M, Gemes G, Sapunar D. Restoration of calcium influx corrects membrane hyperexcitability in injured rat dorsal root ganglion neurons. *Anesth Analg*. 2008; 107(3):1045–1051. [PubMed: 18713927]
33. Hogan QH, McCallum JB, Sarantopoulos C, Aason M, Mynlieff M, Kwok WM, Bosnjak ZJ. Painful neuropathy decreases membrane calcium current in mammalian primary afferent neurons. *Pain*. 2000; 86(1–2):43–53. [PubMed: 10779659]
34. Hudmon A, Schulman H, Kim J, Maltez JM, Tsien RW, Pitt GS. CaMKII tethers to L-type Ca²⁺ channels, establishing a local and dedicated integrator of Ca²⁺ signals for facilitation. *J Cell Biol*. 2005; 171(3):537–547. [PubMed: 16275756]
35. Jagodic MM, Pathirathna S, Joksovic PM, Lee W, Nelson MT, Naik AK, Su P, Jevtovic-Todorovic V, Todorovic SM. Upregulation of the T-type calcium current in small rat sensory neurons after chronic constrictive injury of the sciatic nerve. *J Neurophysiol*. 2008; 99(6):3151–3156. [PubMed: 18417624]
36. Jagodic MM, Pathirathna S, Nelson MT, Mancuso S, Joksovic PM, Rosenberg ER, Bayliss DA, Jevtovic-Todorovic V, Todorovic SM. Cell-specific alterations of T-type calcium current in painful diabetic neuropathy enhance excitability of sensory neurons. *J Neurosci*. 2007; 27(12):3305–3316. [PubMed: 17376991]
37. Kawano T, Zoga V, Gemes G, McCallum JB, Wu HE, Pravdic D, Liang MY, Kwok WM, Hogan Q, Sarantopoulos C. Suppressed Ca²⁺/CaM/CaMKII-dependent K(ATP) channel activity in primary afferent neurons mediates hyperalgesia after axotomy. *Proc Natl Acad Sci U S A*. 2009; 106(21):8725–8730. [PubMed: 19439665]
38. Kim DS, Figueroa KW, Li KW, Boroujerdi A, Yolo T, Luo ZD. Profiling of dynamically changed gene expression in dorsal root ganglia post peripheral nerve injury and a critical role of injury-

- induced glial fibrillary acidic protein in maintenance of pain behaviors [corrected]. *Pain*. 2009; 143(1–2):114–122. [PubMed: 19307059]
39. Kim DS, Li KW, Boroujerdi A, Peter Yu Y, Zhou CY, Deng P, Park J, Zhang X, Lee J, Corpe M, Sharp K, Steward O, Eroglu C, Barres B, Zaucke F, Xu ZC, Luo ZD. Thrombospondin-4 contributes to spinal sensitization and neuropathic pain states. *J Neurosci*. 2012; 32(26):8977–8987. [PubMed: 22745497]
40. Kim SH, Chung JM. An experimental model for peripheral neuropathy produced by segmental spinal nerve ligation in the rat. *Pain*. 1992; 50(3):355–363. [PubMed: 1333581]
41. Kojundzic SL, Puljak L, Hogan Q, Sapunar D. Depression of Ca(2+)/calmodulin-dependent protein kinase II in dorsal root ganglion neurons after spinal nerve ligation. *J Comp Neurol*. 2008; 518(1): 64–74. [PubMed: 19882720]
42. Kostic S, Pan B, Guo Y, Yu H, Sapunar D, Kwok WM, Hudmon A, Wu HE, Hogan QH. Regulation of voltage-gated Ca(2+) currents by Ca(2+)/calmodulin-dependent protein kinase II in resting sensory neurons. *Mol Cell Neurosci*. 2014; 62:10–18. [PubMed: 25064143]
43. Ku WH, Schneider SP. Multiple T-type Ca²⁺ current subtypes in electrophysiologically characterized hamster dorsal horn neurons: possible role in spinal sensory integration. *J Neurophysiol*. 2011; 106(5):2486–2498. [PubMed: 21795620]
44. Li CY, Zhang XL, Matthews EA, Li KW, Kurwa A, Boroujerdi A, Gross J, Gold MS, Dickenson AH, Feng G, Luo ZD. Calcium channel alpha2delta1 subunit mediates spinal hyperexcitability in pain modulation. *Pain*. 2006; 125(1–2):20–34. [PubMed: 16764990]
45. Li L, Rutlin M, Abaira VE, Cassidy C, Kus L, Gong S, Jankowski MP, Luo W, Heintz N, Koerber HR, Woodbury CJ, Ginty DD. The functional organization of cutaneous low-threshold mechanosensory neurons. *Cell*. 2011; 147(7):1615–1627. [PubMed: 22196735]
46. Lirk P, Poroli M, Rigaud M, Fuchs A, Phillip P, Huang CY, Ljubkovic M, Sapunar D, Hogan Q. Modulators of calcium influx regulate membrane excitability in rat dorsal root ganglion neurons. *Anesth Analg*. 2008; 107(2):673–685. [PubMed: 18633052]
47. Lu SG, Zhang XL, Luo ZD, Gold MS. Persistent inflammation alters the density and distribution of voltage-activated calcium channels in subpopulations of rat cutaneous DRG neurons. *Pain*. 2010; 151(3):633–643. [PubMed: 20884119]
48. Luo ZD, Chaplan SR, Higuera ES, Sorkin LS, Stauderman KA, Williams ME, Yaksh TL. Upregulation of dorsal root ganglion (alpha)2(delta) calcium channel subunit and its correlation with allodynia in spinal nerve-injured rats. *J Neurosci*. 2001; 21(6):1868–1875. [PubMed: 11245671]
49. Maneuf YP, Blake R, Andrews NA, McKnight AT. Reduction by gabapentin of K⁺-evoked release of [3H]-glutamate from the caudal trigeminal nucleus of the streptozotocin-treated rat. *Br J Pharmacol*. 2004; 141(4):574–579. [PubMed: 14744819]
50. Martin DJ, McClelland D, Herd MB, Sutton KG, Hall MD, Lee K, Pinnock RD, Scott RH. Gabapentin-mediated inhibition of voltage-activated Ca²⁺ channel currents in cultured sensory neurones is dependent on culture conditions and channel subunit expression. *Neuropharmacology*. 2002; 42(3):353–366. [PubMed: 11897114]
51. Martin SW, Butcher AJ, Berrow NS, Richards MW, Paddon RE, Turner DJ, Dolphin AC, Sihra TS, Fitzgerald EM. Phosphorylation sites on calcium channel alpha1 and beta subunits regulate ERK-dependent modulation of neuronal N-type calcium channels. *Cell Calcium*. 2006; 39(3):275–292. [PubMed: 16406008]
52. McCallum JB, Kwok WM, Mynlieff M, Bosnjak ZJ, Hogan QH. Loss of T-type calcium current in sensory neurons of rats with neuropathic pain. *Anesthesiology*. 2003; 98(1):209–216. [PubMed: 12502999]
53. McCallum JB, Kwok WM, Sapunar D, Fuchs A, Hogan QH. Painful peripheral nerve injury decreases calcium current in axotomized sensory neurons. *Anesthesiology*. 2006; 105(1):160–168. [PubMed: 16810008]
54. McCallum JB, Wu HE, Tang Q, Kwok WM, Hogan QH. Subtype-specific reduction of voltage-gated calcium current in medium-sized dorsal root ganglion neurons after painful peripheral nerve injury. *Neuroscience*. 2011; 179:244–255. [PubMed: 21277351]

55. Nelson MT, Joksovic PM, Perez-Reyes E, Todorovic SM. The endogenous redox agent L-cysteine induces T-type Ca²⁺ channel-dependent sensitization of a novel subpopulation of rat peripheral nociceptors. *J Neurosci*. 2005; 25(38):8766–8775. [PubMed: 16177046]
56. Pan B, Yu H, Park J, Yu YP, Luo ZD, Hogan QH. Painful nerve injury upregulates thrombospondin-4 expression in dorsal root ganglia. *J Neurosci Res*. 2015; 93(3):443–453. [PubMed: 25327416]
57. Park J, Luo ZD. Calcium channel functions in pain processing. *Channels (Austin)*. 2010; 4(6):510–517. [PubMed: 21150297]
58. Patel R, Bauer CS, Nieto-Rostro M, Margas W, Ferron L, Chaggar K, Crews K, Ramirez JD, Bennett DL, Schwartz A, Dickenson AH, Dolphin AC. alpha2delta-1 gene deletion affects somatosensory neuron function and delays mechanical hypersensitivity in response to peripheral nerve damage. *J Neurosci*. 2013; 33(42):16412–16426. [PubMed: 24133248]
59. Perez-Reyes E. Molecular physiology of low-voltage-activated t-type calcium channels. *Physiol Rev*. 2003; 83(1):117–161. [PubMed: 12506128]
60. Pitcher GM, Henry JL. Governing role of primary afferent drive in increased excitation of spinal nociceptive neurons in a model of sciatic neuropathy. *Exp Neurol*. 2008; 214(2):219–228. [PubMed: 18773893]
61. Rigaud M, Gemes G, Barabas ME, Chernoff DI, Abram SE, Stucky CL, Hogan QH. Species and strain differences in rodent sciatic nerve anatomy: implications for studies of neuropathic pain. *Pain*. 2008; 136(1–2):188–201. [PubMed: 18316160]
62. Risher WC, Eroglu C. Thrombospondins as key regulators of synaptogenesis in the central nervous system. *Matrix Biol*. 2012; 31(3):170–177. [PubMed: 22285841]
63. Sapunar D, Ljubkovic M, Lirk P, McCallum JB, Hogan QH. Distinct membrane effects of spinal nerve ligation on injured and adjacent dorsal root ganglion neurons in rats. *Anesthesiology*. 2005; 103(2):360–376. [PubMed: 16052119]
64. Scroggs RS, Fox AP. Multiple Ca²⁺ currents elicited by action potential waveforms in acutely isolated adult rat dorsal root ganglion neurons. *J Neurosci*. 1992; 12(5):1789–1801. [PubMed: 1578270]
65. Simms BA, Zamponi GW. Neuronal voltage-gated calcium channels: structure, function, and dysfunction. *Neuron*. 2014; 82(1):24–45. [PubMed: 24698266]
66. Strobeck MW, Okuda M, Yamaguchi H, Schwartz A, Fukasawa K. Morphological transformation induced by activation of the mitogen-activated protein kinase pathway requires suppression of the T-type Ca²⁺ channel. *J Biol Chem*. 1999; 274(22):15694–15700. [PubMed: 10336467]
67. Sutton KG, Martin DJ, Pinnock RD, Lee K, Scott RH. Gabapentin inhibits high-threshold calcium channel currents in cultured rat dorsal root ganglion neurones. *Br J Pharmacol*. 2002; 135(1):257–265. [PubMed: 11786502]
68. Tang Q, Bangaru ML, Kostic S, Pan B, Wu HE, Koopmeiners AS, Yu H, Fischer GJ, McCallum JB, Kwok WM, Hudmon A, Hogan QH. Ca²⁺(+)-dependent regulation of Ca²⁺(+) currents in rat primary afferent neurons: role of CaMKII and the effect of injury. *J Neurosci*. 2012; 32(34):11737–11749. [PubMed: 22915116]
69. Todorovic SM, Jevtovic-Todorovic V. The role of T-type calcium channels in peripheral and central pain processing. *CNS Neurol Disord Drug Targets*. 2006; 5(6):639–653. [PubMed: 17168748]
70. Torsney C, MacDermott AB. Disinhibition opens the gate to pathological pain signaling in superficial neurokinin 1 receptor-expressing neurons in rat spinal cord. *J Neurosci*. 2006; 26(6):1833–1843. [PubMed: 16467532]
71. Tran-Van-Minh A, Dolphin AC. The alpha2delta ligand gabapentin inhibits the Rab11-dependent recycling of the calcium channel subunit alpha2delta-2. *J Neurosci*. 2010; 30(38):12856–12867. [PubMed: 20861389]
72. Valder CR, Liu JJ, Song YH, Luo ZD. Coupling gene chip analyses and rat genetic variances in identifying potential target genes that may contribute to neuropathic allodynia development. *J Neurochem*. 2003; 87(3):560–573. [PubMed: 14535940]
73. Woodall AJ, Richards MA, Turner DJ, Fitzgerald EM. Growth factors differentially regulate neuronal Cav channels via ERK-dependent signalling. *Cell Calcium*. 2008; 43(6):562–575. [PubMed: 17996937]

74. Wu G, Ringkamp M, Hartke TV, Murinson BB, Campbell JN, Griffin JW, Meyer RA. Early onset of spontaneous activity in uninjured C-fiber nociceptors after injury to neighboring nerve fibers. *J Neurosci*. 2001; 21(8):RC140. [PubMed: 11306646]
75. Wu HE, Gemes G, Zoga V, Kawano T, Hogan QH. Learned avoidance from noxious mechanical stimulation but not threshold semmes weinstein filament stimulation after nerve injury in rats. *J Pain*. 2010; 11(3):280–286. [PubMed: 19945356]
76. Wyatt CN, Page KM, Berrow NS, Brice NL, Dolphin AC. The effect of overexpression of auxiliary Ca²⁺ channel subunits on native Ca²⁺ channel currents in undifferentiated mammalian NG108-15 cells. *J Physiol*. 1998; 510(Pt 2):347–360. [PubMed: 9705988]
77. Zhu Y, Ikeda SR. Modulation of Ca(2+)-channel currents by protein kinase C in adult rat sympathetic neurons. *J Neurophysiol*. 1994; 72(4):1549–1560. [PubMed: 7823085]

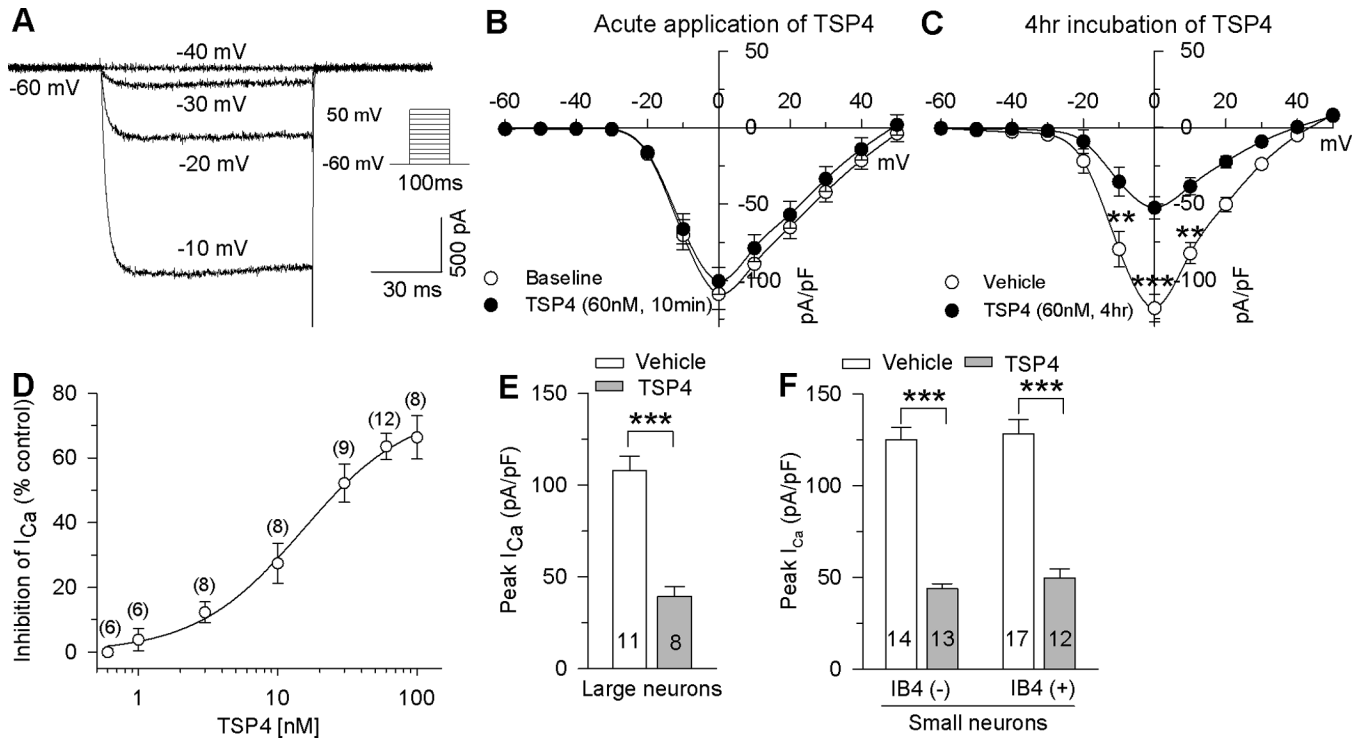


Figure 1. Effects of TSP4 on HVA I_{Ca} in DRG neurons

A, Typical HVA I_{Ca} traces in a small-sized neuron show a threshold for activation at -30 mV and demonstrated little inactivation. The protocol used to evoke currents is shown in the inset. **B**, Acute bath application (10min) of TSP4 had no effect on HVA I_{Ca} ($n = 6$). **C**, 4 hr incubation of TSP4 reduced I_{Ca} , with significant effect measured at depolarization to 0 mV (vehicle control: $n = 42$; TSP4: $n = 33$. $**P < 0.01$, $***P < 0.001$ by 2-way ANOVA, Tukey's post hoc). **D**, Concentration dependence of I_{Ca} inhibition by TSP4 incubation, measured at the peak I_{Ca} for each neuron, revealed an IC_{50} of 15.1 ± 1.2 nM (numbers in the brackets represent the recorded cells for each point). **E, F**, TSP4 non-selectively reduced peak HVA I_{Ca} in large-sized neurons (**E**, over $27\mu\text{m}$ in diameter), and in small-sized neurons (**F**, $15\text{--}27\mu\text{m}$ in diameter) of both the IB4(-) and IB4(+) populations. The numbers in the bars represent the n for group size here and in subsequent figures. $**P < 0.01$ by Student's t test.

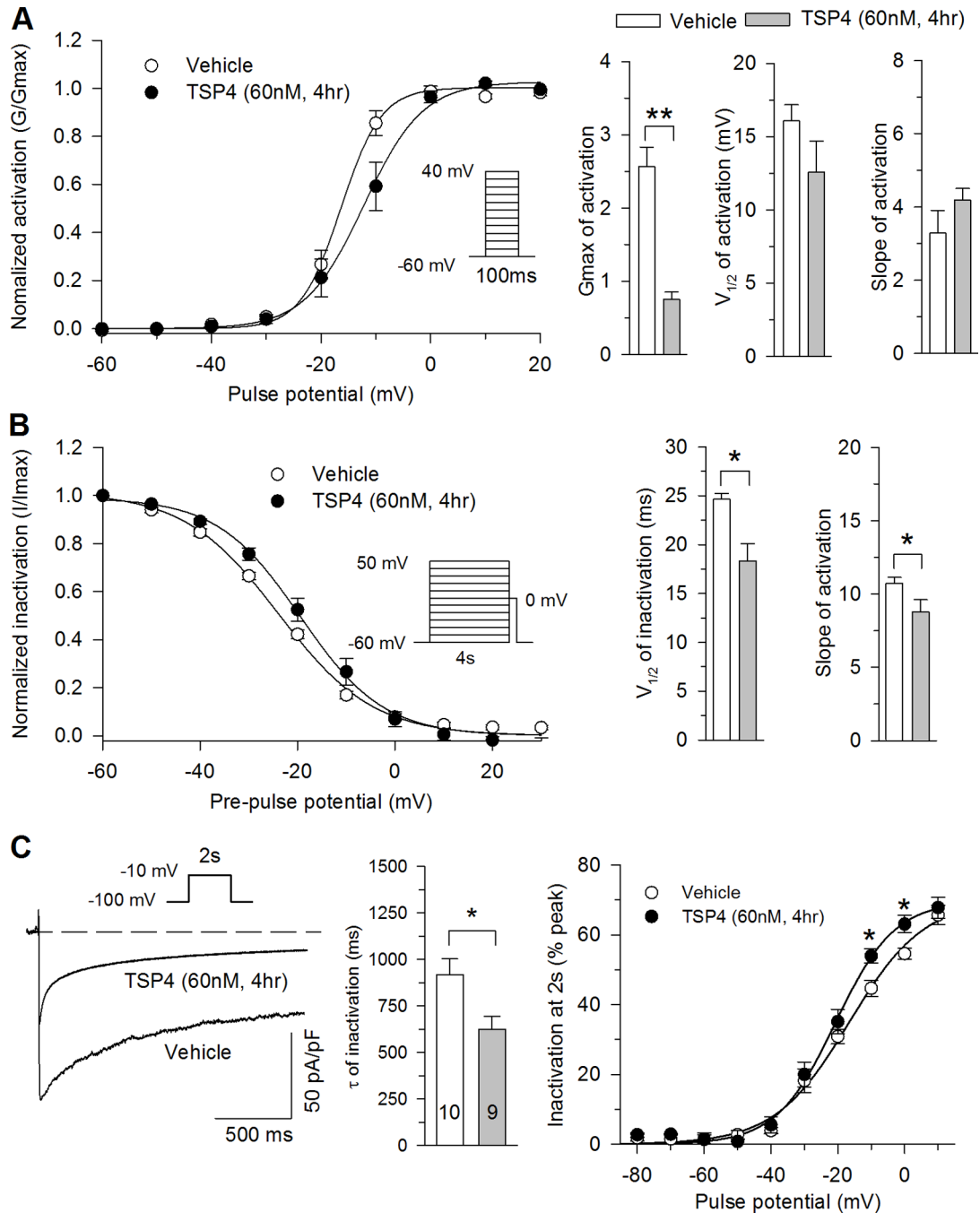


Figure 2. Effects of TSP4 on biophysical properties of HVA VGCCs

A, TSP4 treatment had no effect on activation voltage (left panel). TSP4 decreased G_{max} but not $V_{1/2}$ or slope factors ($n=9$ for control and $n=7$ for TSP4 treatment). **B**, TSP4 treatment shifted the inactivation curve (left panel) to more positive voltages, but had no effect on the slope factor (right panel; $n=7$ for control, $n=6$ for TSP4, * $P < 0.05$ by Student's t test.). **C**, TSP4 increased current inactivation during sustained depolarization from holding at -100 mV, shown in sample traces with depolarization to -10 mV (left panel), τ of inactivation during 2s of persistent depolarization (middle panel) and the ratio of current loss

during 2s of persistent depolarization (right panel; n = 10 for vehicle control, n = 9 for TSP4). * $P < 0.05$ by Student's t test or Tukey post hoc analysis following 2-way repeated measures ANOVA.

Author Manuscript

Author Manuscript

Author Manuscript

Author Manuscript

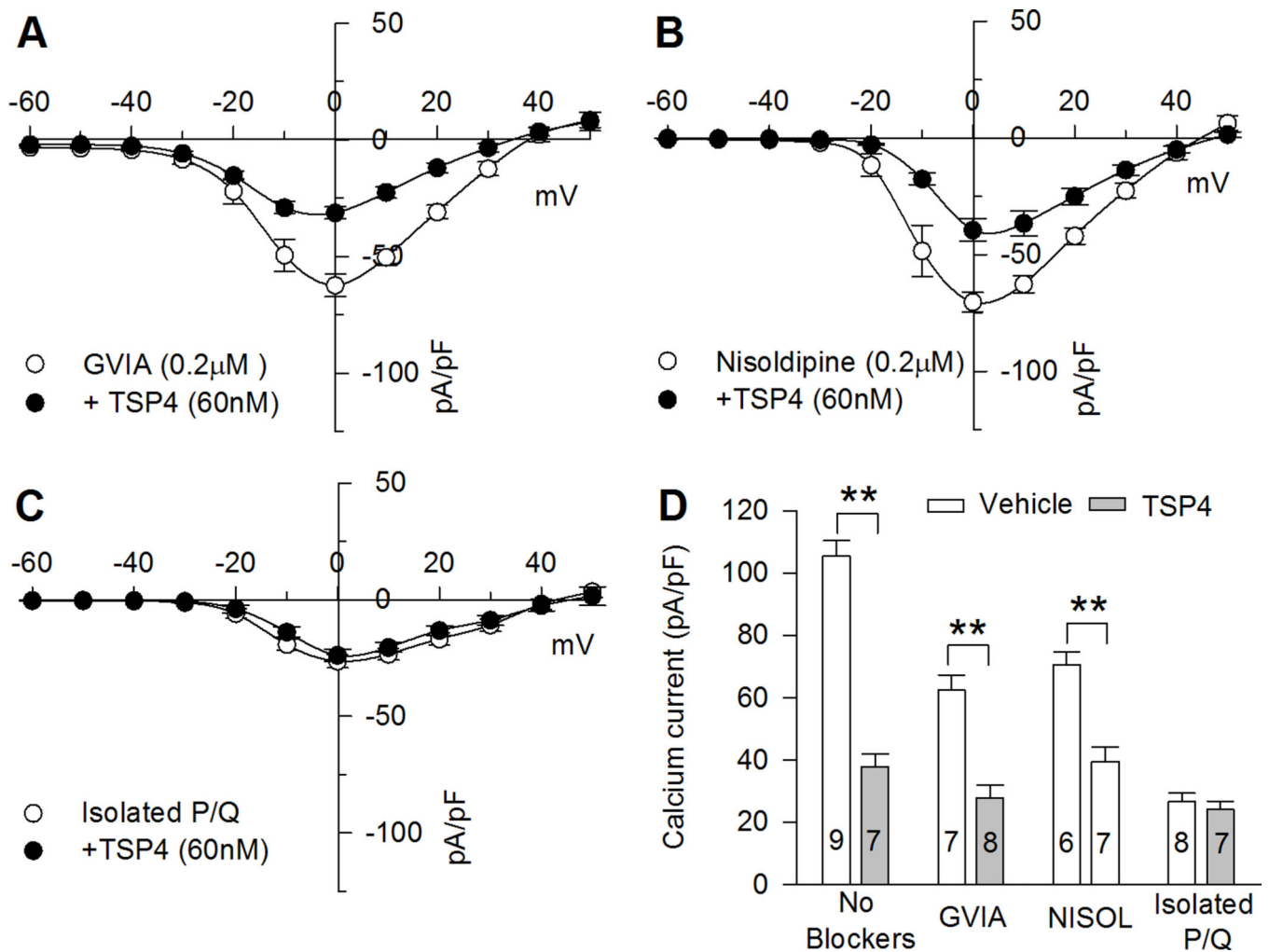


Figure 3. Effects of TSP4 on HVA VGCC subtypes

A, In the presence of N-type VGCCs blocker ω -conotoxin GVIA, TSP4 reduced residual HVA I_{Ca} . **B**, In the presence of L-type VGCCs blocker nisoldipine, TSP4 also reduced HVA residual I_{Ca} . **C**, TSP4 had no effect on isolated P/Q-type I_{Ca} . **D**, Summary data show TSP4 effect on total I_{Ca} and I_{Ca} remaining after block with GVIA and with nisoldipine (NISOL) but no effect on isolated P/Q-type I_{Ca} all measured at 0mV. ** $P < 0.01$ by one-way ANOVA with Tukey's post hoc analysis.

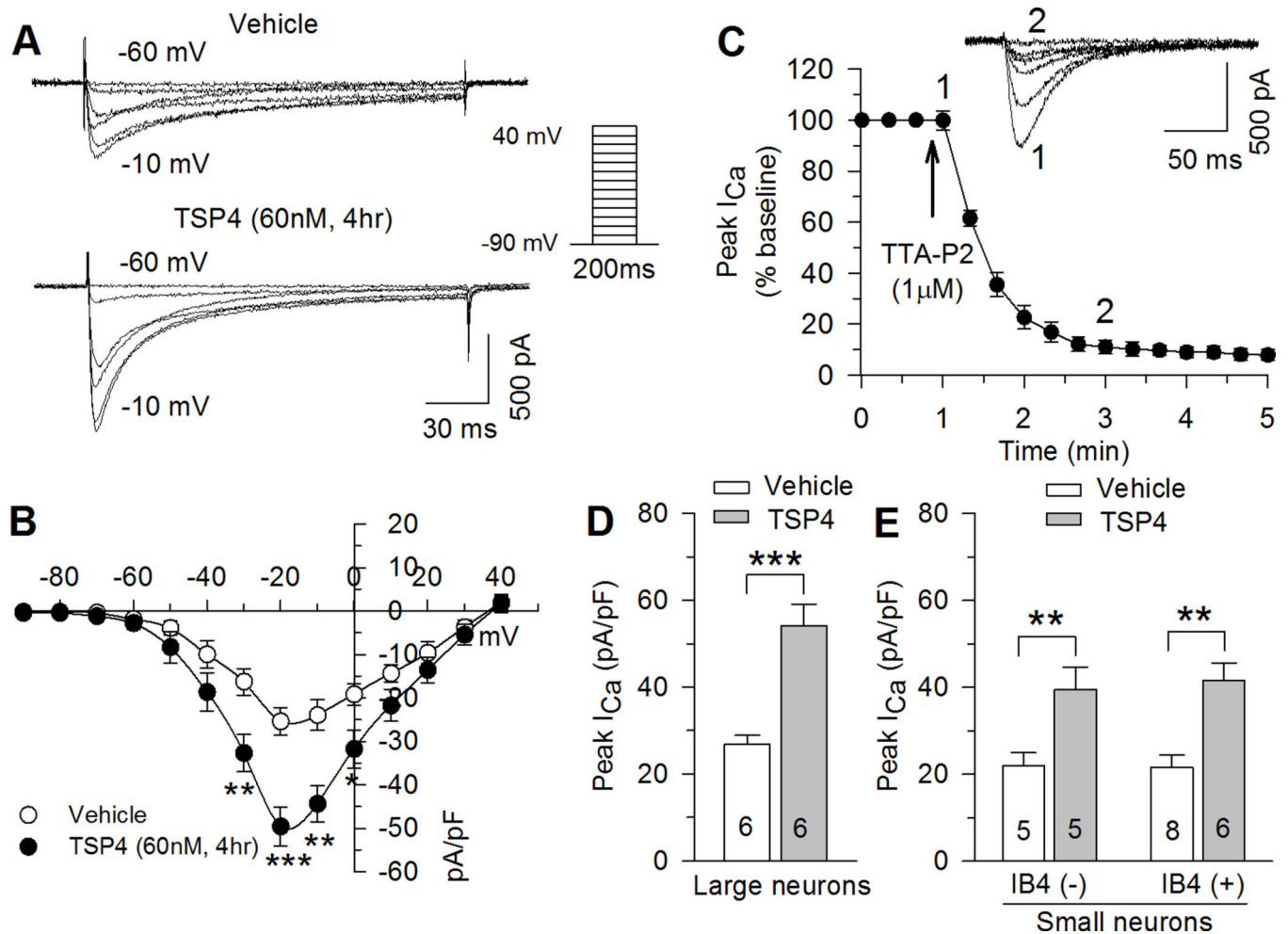


Figure 4. Effects of TSP4 on LVA I_{Ca} in DRG neurons

Sample I_{Ca} traces (**A**) and current-voltage curves (**B**) show LVA I_{Ca} increase during TSP4 treatment (vehicle control: $n = 19$; TSP4: $n = 17$). $*P < 0.05$, $**P < 0.01$, $***P < 0.001$ by 2-way ANOVA with Tukey's post hoc. (**C**) LVA I_{Ca} was blocked by TTA-P2 (top panel: sample traces showing time course of TTA-P2's effects; bottom panel: averaged time data. $n = 4$). (**DE**) TSP4 non-selectively increased LVA I_{Ca} in large-sized neurons (**D**), and in small-sized neurons (**E**) of both the IB4(-) and IB4(+) populations. Means \pm SEM from number of neurons indicated. $**P < 0.01$, $***P < 0.001$ by Student's t test or one-way ANOVA with Tukey's post hoc analysis.

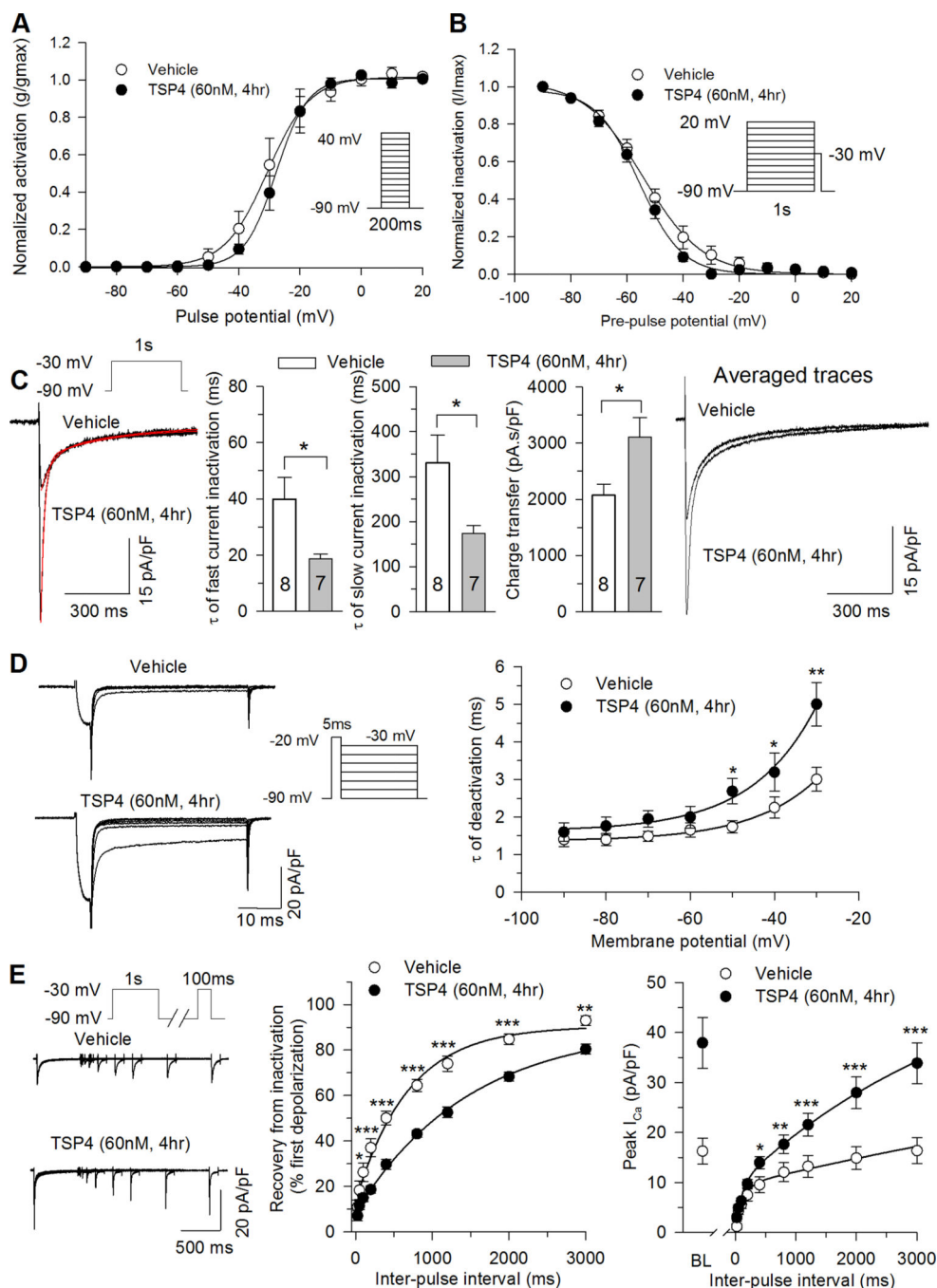


Figure 5. Effects of TSP4 on biophysical properties of LVA VGCCs

TSP4 treatment did not change T-type I_{Ca} voltage dependence of activation (A, $n = 8$ Vehicle control, $n = 7$ TSP4). TSP4 treatment had no effect on steady state inactivation (B, $n = 6$ Vehicle control, $n = 6$ TSP4), but did accelerate inactivation (C, sample traces left panel, and summary data middle panel), including reduced τ for both the fast and slow components of inactivation, while total charge transfer was unaffected and average current density was still greater at all timepoints following the initiation of depolarization (C, right panel). TSP4 reduced the rate of recovery of LVA I_{Ca} from inactivation (D), but the average current

density in TSP4-treated neurons is greater than vehicle controls at all timepoints during recovery (D, right panel, BL: baseline). TSP4 slowed deactivation of LVA I_{Ca} from activation (**E**, n = 7 Vehicle control, n = 7 TSP4). * $P < 0.05$, ** $P < 0.01$, *** $P < 0.001$, Tukey post hoc analysis following 2-way repeated measures ANOVA.

Author Manuscript

Author Manuscript

Author Manuscript

Author Manuscript

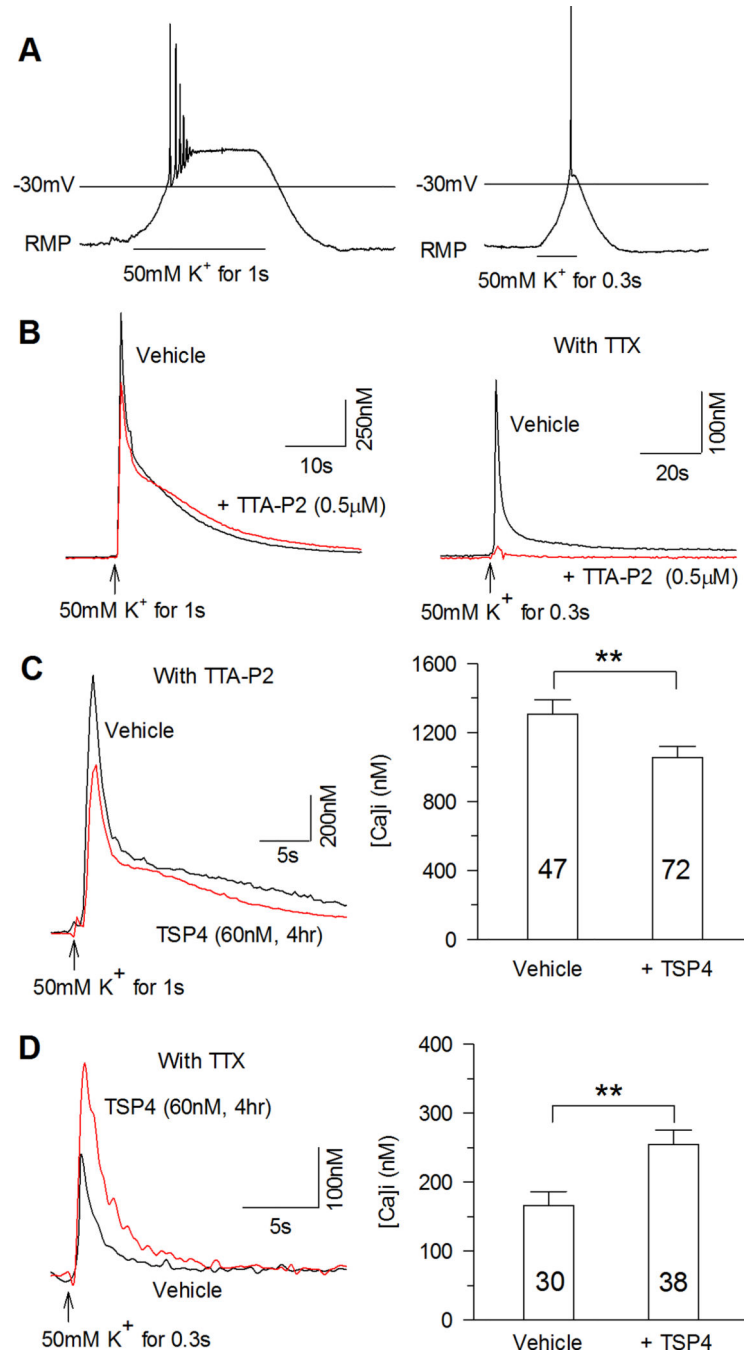


Figure 6. Effects of TSP4 on intracellular calcium transient in DRG neurons

A, Bath application of 50 mM K^+ for 1 s depolarized sensory neurons to -12 ± 2 mV (left panel, $n = 3$), and 50 mM K^+ for 0.3 s depolarized neurons to -31.3 ± 2.9 mV (right panel, $n = 3$). **B**, 1 s depolarization induced intracellular Ca^{2+} transient that was resistant to the T-type Ca^{2+} channel blocker TTA-P2 (left panel, typical of $n = 8$), while the intracellular calcium transient induced by 50 mM K^+ for 0.3 s could be blocked by TTA-P2 (right panel, typical of $n = 10$). To avoid membrane depolarization from AP generation, TTX (1 μ M) was added during subsequent recordings. **C**, TSP4 treatment reduced intracellular Ca^{2+} transients

induced by 50 mM K^+ for 1s. **D**, In contrast, TSP4 treatment increased intracellular Ca^{2+} transients induced by 50 mM K^+ for 0.3s. ** $P < 0.01$ by Student's t test.

Author Manuscript

Author Manuscript

Author Manuscript

Author Manuscript

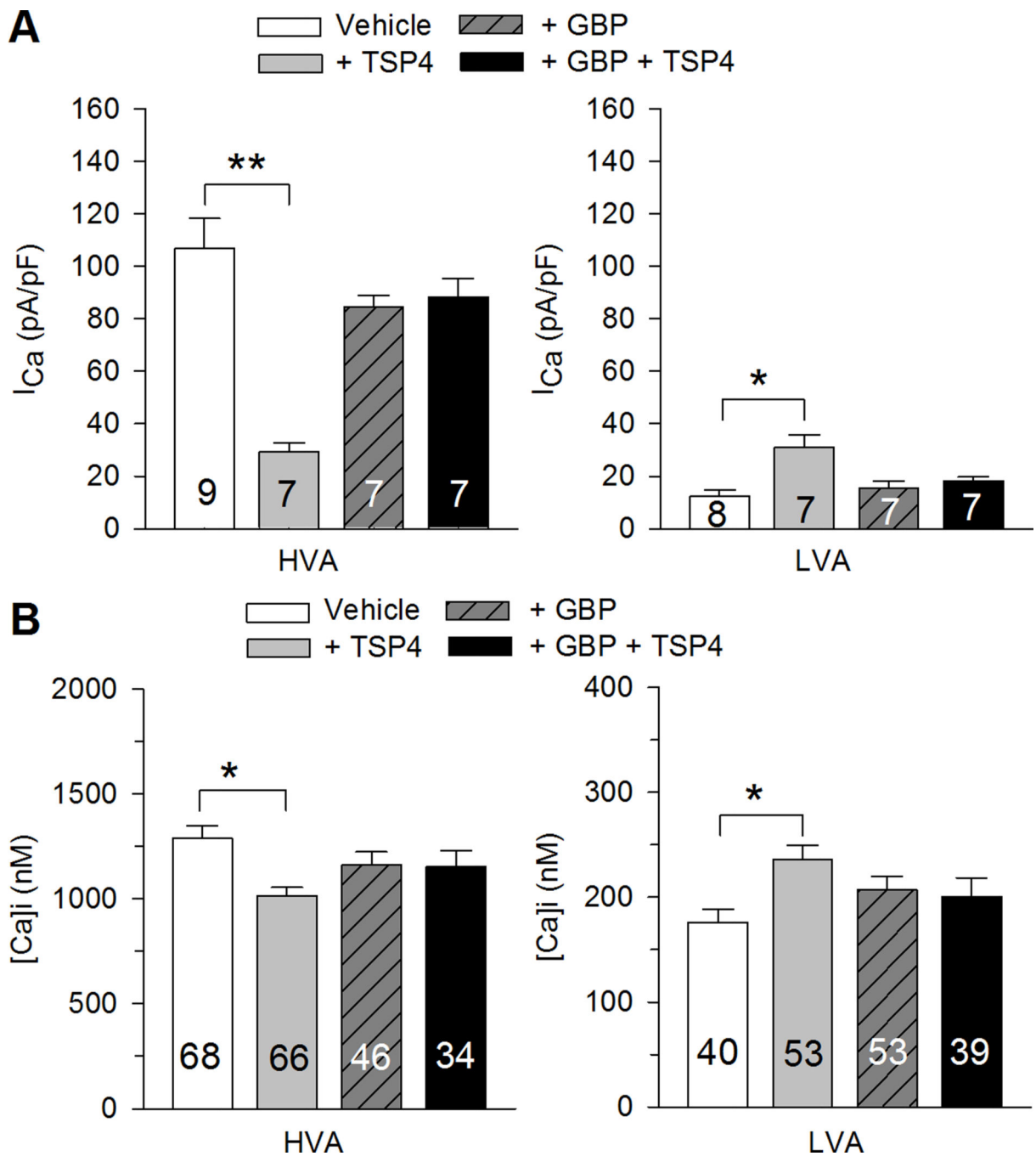


Figure 7. Gabapentin (GBP) blocks effects of TSP4 on I_{Ca} and the intracellular Ca^{2+} transient
A, TSP4-induced reduction of HVA I_{Ca} (left panel) and elevation of LVA I_{Ca} (right panel) were eliminated by GBP. **B**, Similarly, GBP blocked effects of TSP4 on the intracellular Ca^{2+} transient through HVA channels activated by 1s 50mM K^+ depolarization and LVA Ca^{2+} channels activated by 0.3s 50mM K^+ depolarization (Veh – Vehicle; * $p < 0.05$, ** $p < 0.01$ for planned comparison (Veh vs. GBP, Veh vs. TSP4, GBP vs. GBP+TSP4, TSP4 vs. G+TSP4) by t-test, with Bonferroni compensation for multiple comparisons.

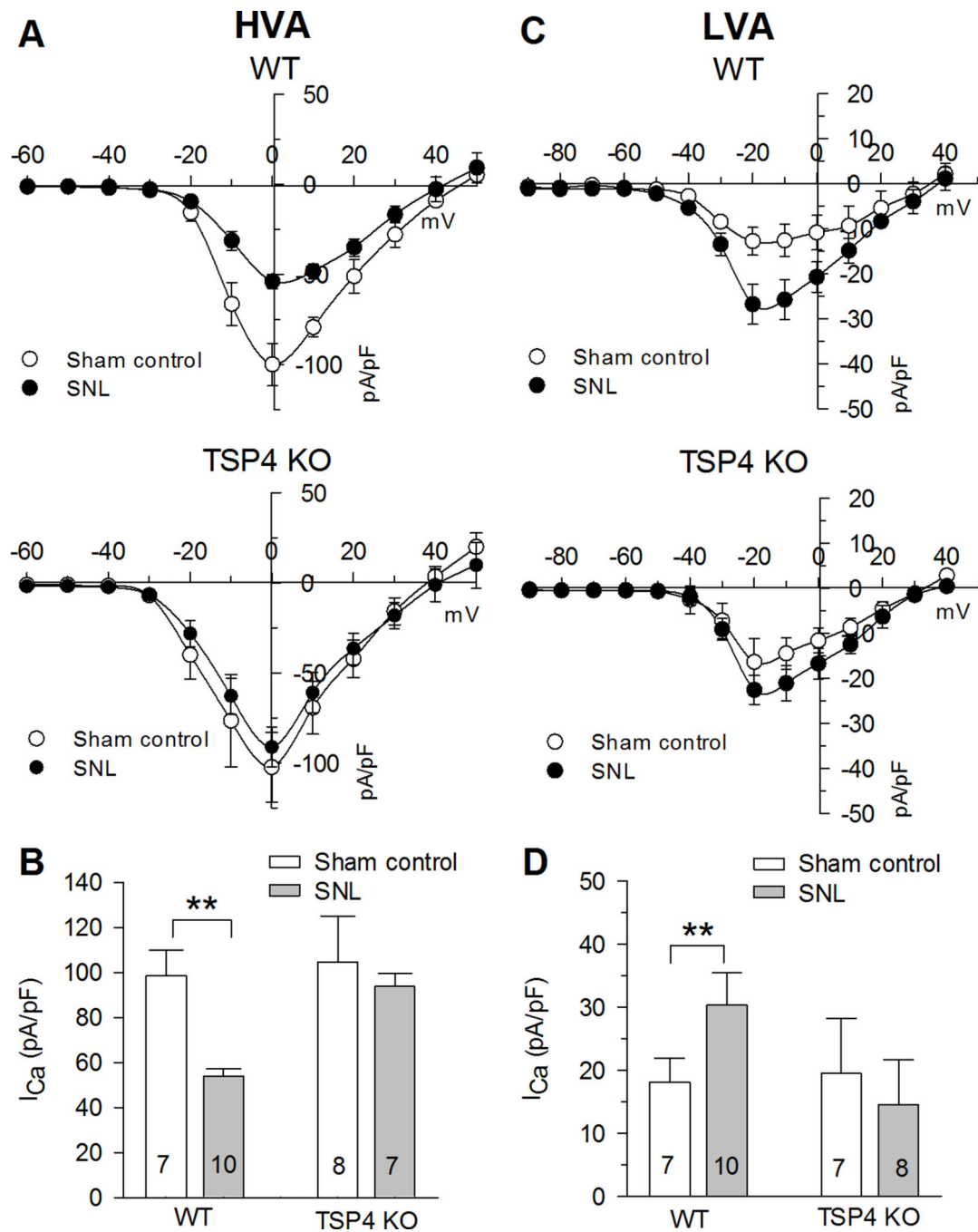


Figure 8. TSP4 knockout (KO) eliminates influence of nerve injury on I_{Ca} after injury
AB SNL injury resulted in reduced HVA I_{Ca} in TSP4 WT mice not in TSP4 KO mice. **CD** SNL injury resulted in increased LVA I_{Ca} in TSP4 WT mice not in TSP4 KO mice. * $P < 0.05$, ** $P < 0.01$ by two-way ANOVA with Tukey's post hoc analysis.

